Peroxidative Oxidation of Lignin and a Lignin Model Compound by a Manganese SALEN Derivative

Stephen D. Springer,[1] Jian He,[2] Megan Chui,[1] R. Daniel Little,[1] Marcus Foston,[2,*] and Alison Butler,[1,*]

[1] Department of Chemistry and Biochemistry, University of California, Santa Barbara, CA 93106-9510, USA

[2] Department of Energy, Environmental & Chemical Engineering, Washington University in St. Louis, St. Louis, MO 63130, USA

*Corresponding authors

butler@chem.ucsb.edu

mfoston@wustl.edu

ABSTRACT The manganese catalyst, (1R,2R)-(-)-[1,2-cyclohexanediamino-N,N'-bis(3,5-di-t-butylsalicylidene)]manganese (III) chloride, was used to activate H_2O_2 to oxidize organosolv lignin and a lignin model compound. Oxidation of the β-O-4 lignin model substrate 1-(4-

hydroxy-3-methoxyphenyl)-2-(2-methoxyphenoxy)propane-1,3-diol (320.3 m/z) and Poplar organosolv lignin resulted in both fragmentation and polymerization processes, likely via phenoxy radical formation. Matrix-assisted laser desorption/ionization (MALDI)-time-of-flight (TOF) mass spectrometry (MS) of the reaction products from the β-O-4 model substrate show oligomers of the substrate with masses of 661.192, 979.355, and 1297.466 m/z that correspond to a dimer, trimer, and tetramer of the β-O-4 model substrate respectively. Nuclear magnetic resonance (NMR) shows the formation of 5-5 diphenyl and 4-O-5 linkages in the β-O-4 model substrate oxidation products. Gel permeation chromatography (GPC) detected three peaks, corresponding to the β-O-4 model substrate and its oligomers. Products from the Mn-catalyzed oxidation of Poplar organosolv lignin by H_2O_2 were analyzed by GPC, ^{31}P NMR, and ^{13}C NMR. GPC showed an increase by approximately four in the number-average molecular weight of organosolv lignin upon oxidation. NMR shows that polymerization occurs at positions consistent with phenoxy radical coupling; where the observed changes in guaiacyl subunit chemical shifts are most likely due to the formation of 5-5 biphenyl linkages.

Keywords: Lignin, Chemical feedstock, Peroxidative Oxidation, Manganese Catalyst, Breakout products, Polymerization

Introduction

   The search for alternatives to petroleum-derived chemicals and fuels has taken on increased importance in recent years.[1] Lignocellulosic biomass is an attractive source of renewable fuels and chemicals with a potentially smaller carbon footprint than petroleum-derived products.[2] Lignin is a large, complex, and heterogeneous macromolecule that is of particular interest

because it is an abundant and unique source of electron-rich aromatic carbon that is not easily generated from other sustainable resources such as proteins or carbohydrates (Figure 1).[2] Products from the depolymerization of lignin are envisioned as precursors and platform chemicals for the downstream production of not only commodity chemicals but also value-added fine chemicals such as pharmaceuticals.[3-5] Critically, however, any process used for the conversion of lignin into such value-added products must perform selective depolymerization reactions, leaving the natural aromaticity intact. Current, biorefinery models employ energy intensive and high temperature processes to depolymerize lignocellulosic biomass or lignin to produce bio-oil.[6-8] Despite recent advances in the thermo-catalytic processing of lignin, transforming lignin into higher value chemicals is very challenging because of its structural diversity, the high temperatures required to overcome its inherent recalcitrance, and the propensity of its depolymerization products to undergo a complex series of secondary (unwanted) reactions at elevated temperatures. To date, many processes using lignin generate complex and varied product distributions that are not amenable to the cost-effective isolation or extraction of any one value-added compound.[9, 10]

The major lignin monomers (e.g., monolignols) consist of coniferyl alcohol, sinapyl alcohol, and coumaryl alcohol, corresponding to guaiacyl (G), syringyl (S), and *p*-hydroxyphenyl (H) groups respectively, with lignin.[11] Polymerization of these lignin monomers in the cell wall is achieved through coupling of phenoxy radicals generated by enzymes, such as peroxidases, laccases, polyphenol oxidases, and coniferyl alcohol oxidase, etc.[11] Delocalization of phenoxy radicals allows the coupling reaction to occur at multiple sites leading to the heterogeneous bonding arrays found in lignin, including many different ether and carbon-carbon linkages.[11] Lignin is a very stable polymer due to its inter-monomer linkage stability, substructural

heterogeneity, and overall hydrophobicity, thus very few biological systems have the capability to degrade it.[12] In fact, the structure of lignin evolved over millions of years as part of plant defensive mechanisms, specifically to resist cell wall degradation from both biotic and abiotic environmental factors.
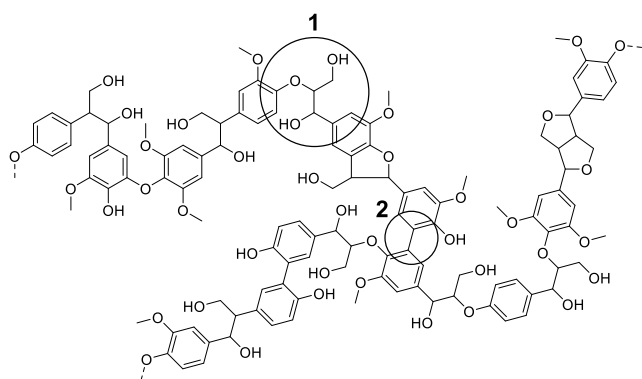

Figure 1. Depiction of structural features of lignin, highlighting a β-O-4 linkage (**1**) and bi-phenyl 5-5 bond (**2**) circled.

In contrast to the laccases and peroxidases used by vascular plants to synthesize lignin, white rot fungi use laccases and peroxidases to oxidatively degrade lignin.[13, 14] Manganese peroxidase (MnP) is an Fe(III) heme lignin peroxidase that generates Mn(III) bound by small organic acids.[15, 16] This Mn(III) complex serves as a redox mediator that diffuses into biomass, oxidizing terminal phenolic groups on lignin into phenoxy radicals.[14] Generation of phenoxy radicals leads to lignin decomposition during fungal growth. Wood and grasses treated with MnP have been shown to degrade slowly, releasing CO_2, water-soluble carbohydrate fragments, and low-molecular weight aromatic compounds.[17-19] Oxidation of lignin model compounds by MnP have been shown to release certain potential value added chemicals such as vanillin and vanillyl alcohol.[20]

The function of these lignin-oxidizing fungal enzymes suggests a bio-mimetic approach for oxidative lignin depolymerization. Manganese porphyrins immobilized on clay have been successfully employed to breakdown lignin model compounds and Kraft lignin producing both fragmentation products and oxidation of the aromatic ring to benzoquinones.[21, 22] When the redox mediator 1-hydroxybenzotriazole was included, it increased activity without changing the product distribution.[22] Cobalt complexes of *N,N'*-bis(salicylidene) ethylenediamine (SALEN) derivatives have also been investigated as catalysts for lignin and lignin model compound degradation.[23-25] Our approach has been to investigate a Mn-SALEN complex in peroxidative oxidation of lignin and lignin model compounds.

We report herein that the Mn-SALEN catalyst, (1R,2R)-(-)-[1,2-cyclohexanediamino-N,N'-bis(3,5-di-t-butylsalicylidene)]manganese (III) chloride, also known as the Jacobsen's catalyst (Figure 2),[26] peroxidatively oxidizes organosolv lignin and the β-O-4 model substrate, 1-(4-hydroxy-3-methoxyphenyl)-2-(2-methoxyphenoxy)-propane-1,3-diol (Figure 2). The oxidation results in both the partial fragmentation of the β-O-4 model substrate, as well as polymerization of the β-O-4 model substrate and the organosolv lignin, with polymerization being the dominate pathway under our conditions. These results are consistent with the generation of phenoxy radicals, and suggest further that much remains to be discovered about the biological degradation of lignin.
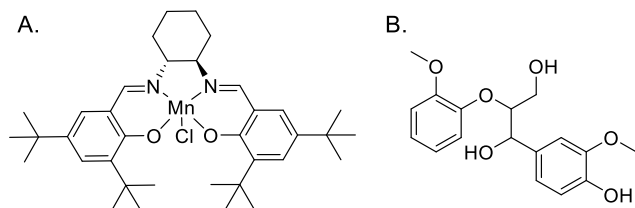

A.   B.

Figure 2. A. The Mn SALEN catalyst, (1R,2R)-(-)-[1,2-cyclohexanediamino-N,N'-bis(3,5-di-t-butylsalicylidene)]manganese (III) chloride. **B.** The β-O-4 model substrate, 1-(4-hydroxy-3-methoxyphenyl)-2-(2-methoxyphenoxy)-propane-1,3-diol.

Methods

General catalytic oxidation conditions.

All oxidation reactions were homogeneous and were run using the Mn catalyst, (1R,2R)-(-)-[1,2-cyclohexanediamino-N,N'-bis(3,5-di-t-butylsalicylidene)]manganese (III) chloride, purchased from Strem Chemicals™. Reactions were carried out in EtOH:H_2O (1:1) at room temperature. H_2O_2 was standardized based on the oxidation of iodide, and was added via syringe pump (Sage ATI Orion 361) to the reaction vial.[27] The substrates used included a β-O-4 phenolic model compound (Scheme S1) and Poplar organosolv lignin. The ratio and concentration of substrate, catalyst, and H_2O_2 were varied depending on the experiment, as described in the text. Product mixtures prepared for analysis were treated with Bio-Rad Chelex, an ion-exchange resin composed of a styrene-divinylbenzene co-polymer containing iminodiacetic acid groups. The Bio-Rad Chelex was used to remove the Mn-catalyst from the product mixture

Oxidation of the β-O-4 lignin model compound for gas chromatography–mass spectrometry (GC-MS) analysis.

The β-O-4 model substrate was oxidized using H_2O_2 activated by the Mn catalyst. The resulting products were prepared for GC-MS analysis as follows: 10 mM β-O-4 model substrate and 1 mM catalyst (10 mol%) were allowed to react with 100 mM H_2O_2 in 1 mL of EtOH:H_2O (1:1) at room temperature; an aliquot was removed once every h for 5 h and a final aliquot was taken after 24 h. Reaction products were passed through a silica gel column to remove the

catalyst prior to analysis using GC-MS. The catalyst-free eluent was evaporated using a N_2 stream and the residue was derivatized using 25 μL N,O-bis(trimethylsilyl)trifluoroacetamide (BSTFA) and 25 μL of pyridine. The internal standard, 3,4-dimethoxytoluene (10 mM), was added during the derivatization of the reaction products.

Oxidation of the β-O-4 lignin model compound for NMR, GPC, and MALDI analysis.

Oxidation of the β-O-4 lignin model compound was achieved by treating 40 mg of the β-O-4 model substrate (41 mM) with 80 mM of H_2O_2 (added over 3 h by syringe pump) and 1 mM of the Mn catalyst (2.4 mol%) in 3 mL of EtOH:H_2O (1:1) at room temperature. After 3 h, the reaction mixture was passed through a Bio-Rad Chelex column (100-200 mesh) to remove the catalyst. Ethanol was removed using a N_2 stream; water was removed by lyophilization. The dried reaction products were re-dissolved in the appropriate solvent (see NMR methods section for detail) for NMR or GPC analysis. Aliquots (50 μL) were taken before and after catalyst removal for MALDI-TOF MS analysis.

Samples oxidized for MALDI-TOF MS analysis were prepared as follows: 50 mM of the β-O-4 model substrate was allowed to react with 100 mM of H_2O_2 (added over 1 h by syringe pump) and 0.1 mM of Mn catalyst (0.2 mol%) in 1 mL of EtOH:H_2O (1:1) at room temperature. Reaction products were then added to the MALDI matrix without further workup.

Oxidation of organosolv lignin.

Poplar organosolv lignin was oxidized by H_2O_2 activated by the Mn catalyst as follows: 60 mg of organosolv was treated with 100 mM H_2O_2 (added by syringe pump over 3 h) and activated by the manganese catalyst (1 mM) in 3 mL of solvent (2 EtOH : 1 H_2O) at room temperature. After 3 h, the products were passed through a Bio-Rad Chelex column (100-200 mesh) to remove the catalyst. Ethanol was removed using a N_2 stream; water was removed by lyophilization. The

dried reaction products were re-dissolved in the "appropriate solvent" for NMR or GPC analysis. Two organosolv lignin control were used for comparison, one was worked up following the same protocol as the oxidized organosolv lignin and one was left untreated.

Gas chromatography–mass spectrometry (GC-MS) of the β-O-4 lignin model compound reaction products.

GC-MS experiments were performed on a Varian 3900 (GC) Saturn 2100T (MS) using a Varian Factorfour™ VF-5ms capillary column (30 m x 0.25 mm 0.25 μm). The injection port was held at 250 °C and the initial oven temperature was maintained 50 °C; after two minutes the oven temperature was ramped to 300 °C over 28 minutes. Helium was used as the carrier gas at a constant flow rate of 1 mL/min.

Matrix Assisted Laser Desorption/Ionization Time of Flight Mass Spectrometry (MALDI-TOF MS) of the β-O-4 lignin model reaction products.

Dissolved products obtained from different β-O-4 model substrate oxidation reactions, described above, were diluted 1:10 and 1:5 (v/v) in a 100 μL eppendorf tube, using a 10 μL pipette, with a saturated α-cyano-4-hydroxycinnamic acid matrix solution consisting of 1:1 acetonitrile:H_2O 0.1% TFA and 0.1 mM NaI. Then 1 μL of the resulting solution was placed on the MADLI plate. MALDI-TOF-MS was carried out on a Bruker Microflex LRF, calibrated from a least squares fit of the Bruker peptide calibration standard II™.

Gel permeation chromatography (GPC) of organosolv lignin reaction products.

Before GPC was carried out, lignin samples were acetylated according to a slightly modified published procedure to facilitate complete dissolution in the chromatography solvent, tetrahydrofuran (THF).[28] Thus, the dried lignin (15 mg) was dissolved in a 1:1 (v/v) acetic anhydride/pyridine mixture (2.00 mL) and stirred at room temperature overnight. Anhydrous

ethanol (5 mL) was then added, and after 30 min, the solvent was removed by rotary evaporation. The residue was washed with ethanol and evaporated under reduced pressure three times until the acetic acid and pyridine was removed from the product (as determined by the absence of additional chromatographic peaks). The lignin acetate was then dissolved in THF (~10 mg/mL) and filtered through a 0.45-μm nylon membrane filter. GPC analysis was carried out using a Waters e2695 system with a 2489 Å ultraviolet detector and a 2414 Å refractive index detector on a three-column sequence of Waters™ Styragel columns (HR0.5, HR1, and HR3). THF was used as eluent, and the flow rate was 1.0 mL/min. Six narrow (polydispersity index of 1.1) polystyrene standards (0.68, 1.25, 3.47, 9.13, 17.6, and 34.8 kg/mol), diphenylmethane, and toluene were used to construct a relative, polynomial calibration curve.

Nuclear Magnetic Resonance (NMR) of the β-O-4 lignin model and organosolv lignin reaction products.

For ^{1}H, ^{13}C, and ^{1}H-^{13}C heteronuclear single quantum coherence (HSQC) NMR, ~50 mg of sample was added into a dry 2-dram vial with 0.5 mL DMSO-d_6. The mixture was stirred for several hours until the solids were completely dissolved. The solution was transferred into a 5 mm NMR tube and back-filled with argon. ^{1}H NMR experiments (45° pulse) were conducted using a Varian Inova 300 MHz spectrometer at 298K with a 2s recycle delay and 32 scans. 2D HSQC correlation NMR spectra were conducted using a Varian Inova 600 MHz spectrometer at 313K. The HSQC analysis was performed using a standard gradient enhanced HSQC (gChsqc_BB) pulse sequence (with a 90° pulse, 0.11 acquisition time, a 1.5-s recycle delay, a J_{C-H} of 145 Hz, and the acquisition of 256 slices and 128 scans. HSQC NMR assignments were carried out according to Kim et al.[29] ^{13}C NMR inverse gated experiments (90° pulse) were conducted using a Varian Inova 300 MHz spectrometer at 313K with a 12 s recycle delay

and 8K scans. ^{13}C NMR assignments and analysis was accomplished in a manner analogous to that used by Capanema et al.[30] An Attached Proton Test (APT) experiment was conducted using a Varian Inova 300 MHz spectrometer at 313K with a 10 s recycle delay and 5K scans.

^{31}P NMR spectra were acquired after *in situ* derivatization under argon of the lignin samples with 2-chloro-4,4,5,5-tetramethyl-1,3,2-dioxaphospholane (TMDP). Anhydrous pyridine and deuterated chloroform (Py/CDCl$_3$, 1.6/1.0 v/v) was used along with a relaxation agent, chromium(III) acetylacetonate, and an internal standard, N-hydroxy-5-norbornene-2,3-dicarboximide. The conditions for ^{31}P NMR inverse gated spectral acquisition on a 300 MHz Varian Unity Plus NMR were as follows: a 90° pulse angle, 15 s pulse delay, and 256 scans at 298K. ^{31}P NMR assignments and the analysis were accomplished in a manner analogous to that used by Samuel et al.[28, 31, 32]

Results/Discussion

Mass spectral analysis of the β-O-4 lignin model oxidation products.

The product mixture of H$_2$O$_2$ oxidation of the β-O-4 model substrate catalyzed by (1R,2R)-(-)-[1,2-cyclohexanediamino-N,N'-bis(3,5-di-t-butylsalicylidene)]manganese (III) chloride, was analyzed by GC-MS after derivatization by the silylation agent N,O-bis(trimethylsilyl)trifluoroacetamide (BSTFA) (Figure 3). The area under each product peak in the chromatogram was normalized to the area of a known concentration of the internal standard, 3,4-dimethoxytoluene (Table S1). The amount of oxidant used in GC-MS experiments was optimized for complete substrate conversion (10 mol eq.), while in experiments for NMR, MALDI, and GPC studies, only 2 mol eq. of oxidant was used to investigate the more interesting case of incomplete substrate conversions.

Under the conditions of the time course experiment described in the methods section, the GC-MS showed 91% of the β-O-4 model substrate was consumed, while producing a ~5% apparent yield of GC-MS-detectable products (Figure 3). Over the course of the experiment, a continuous increase in product formation is seen, with the exception of product 2, which after the initial increase in relative abundance in the first hour, remains steady thereafter (Table S1). The absence of sufficient product to account for the full mass balance could be due to over-oxidation resulting in the formation of CO_2 and low molecular weight carboxylic acids,[33-35] as well as polymerization of the substrate. Radical polymerization is known to occur for lignin model compounds when phenoxy radicals are generated through oxidation of terminal phenols.[25, 36, 37]

Substrate consumed

91%

Product 1   Product 2   Product 3

Relative abundance of products compared to
the starting substrate
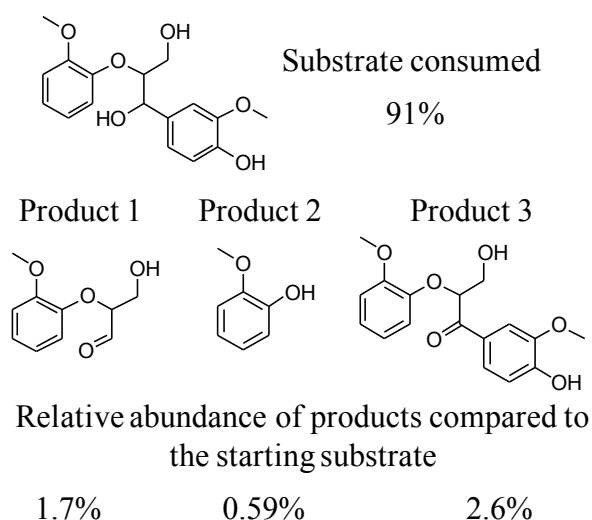
1.7%   0.59%   2.6%

Figure 3. Relative abundance of substrate and products compared to the internal standard 3,4-dimethoxytoluene. Products 1 and 3 are putatively assigned by mass. Product 2, was confirmed by comparison to an authentic sample of 2-methoxy phenol. The relative abundance of each compound was determined by dividing the product peak area by the internal standard peak area.

Polymerization of the β-O-4 model substrate most likely occurs through a radical-initiated pathway by hydrogen atom abstraction or oxidation of the phenol subunit. Polymerization via

phenoxy radical coupling would result in the formation of bonds analogous to the 5-5 or 4-O-5 lignin linkages (Figure 4). Potential polymerization products with their (m/z + Na$^+$) values are also shown. Masses observed in the MALDI-TOF MS spectrum correspond to dimers, trimers and tetramers of the substrate that are consistent with 5-5 or 4-O-5 bond formation from radical coupling (Figure S16).
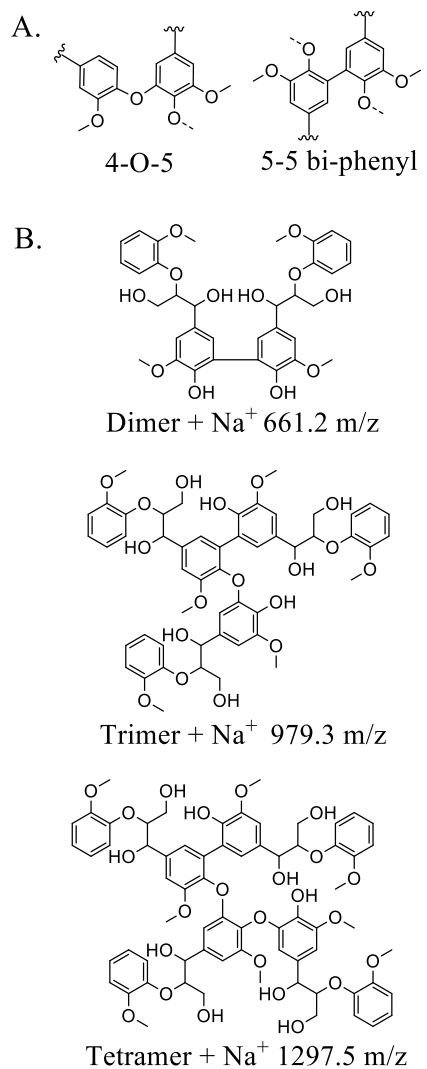
A.

4-O-5   5-5 bi-phenyl

B.

Dimer + Na$^+$ 661.2 m/z

Trimer + Na$^+$ 979.3 m/z

Tetramer + Na$^+$ 1297.5 m/z

Figure 4. A. 4-O-5 and 5-5 bi-phenyl lignin cross coupling linkages. B. Possible β-O-4 model substrate polymerization products from a phenoxy radical coupling mechanism.

Gel permeation chromatography (GPC) of the reaction product mixture after Chelex treatment, shows three resolvable peaks that represent the β-O-4 model substrate and its oligomers (Figure S2). Integration of GPC peaks shows a 7:3:1 ratio of β-O-4 model substrate to its dimer and trimer in the product mixture after Chelex treatment. MALDI-TOF MS of the reaction products before Chelex treatment have peaks corresponding to the dimer, trimer, and tetramer of the β-O-4 model substrate by mass; however, after Chelex treatment the tetramer was no longer observed, indicating that the Chelex work up procedure removed some of the polymerization products (Figure S3).

NMR analysis of the β-O-4 model substrate oxidation products.

^{1}H and ^{13}C NMR analysis of the β-O-4 model substrate reaction products after Chelex treatment (Figures S4 and S5) indicate that dimerization of the β-O-4 model substrate occurs by formation of 5-5 diphenyl linkage, likely via phenoxy radical coupling. Peak assignments and integration for the ^{1}H NMR spectra are provided in Table 1. The proper ratio of protons corresponding to the α-, β- and γ-positions (defined in Figure S4) indicates that the oxidation is not modifying the aliphatic region of the β-O-4 model substrate (peak assignments were made in accord with reported chemical shifts for lignin model compounds[38] and heteronuclear single quantum coherence (HSQC) NMR seen in Figure S6). Integration of the hydroxyl protons at the α- and γ-position suggest that oxidation and polymerization does not modify them; however, a ~40% decrease in the integration (with respect to β-O-4 model substrate) of the hydroxyl proton located at 4-postion of the β-O-4 model substrate does suggest polymerization is partially mediated at those phenolic sites. This information along with the fact that the integration of the methoxy position is less than the predicted value, suggests that polymerization is also occurring

through transetherification, forming a 4-O-5 linkage and methanol (attributed to the methyl group of the aromatic methoxy)..

The ^{13}C NMR spectrum of the β-O-4 model substrate reaction products shows the appearance of a peak at 128.2 ppm, not seen in the ^{13}C spectrum of the β-O-4 model substrate, which has been attributed to a carbon positioned at the 5-5 diphenyl linkage based on reported ^{13}C chemical shifts for lignin model compounds[38] containing 5-5 diphenyl linkages. Attached proton test (APT) NMR spectra confirmed that the peak at 128.2 ppm is a quaternary carbon (Figure S7). Peak assignments and integration for the ^{13}C NMR spectra are in Table 1 (peak assignments were made with reported chemical shifts for lignin model compounds,[38] HSQC NMR in Figure S6, and APT NMR in Figure S7). Based on the integration of the peak at 128.2 ppm, approximately 40% of the carbons at the 5-position in the β-O-4 model substrate are converted to 5-5 carbons upon dimerization by the Mn-catalyst. Also, the integration of peaks attributed to methoxy carbons is lower than the predicted value for the β-O-4 model substrate. This also confirms that polymerization occurs through the formation of 4-O-5 linkages as described above.

In summary, MALDI-TOF and NMR analyses indicate that the primary mode of reaction of the β-O-4 model substrate induced by the Mn-catalyst and H_2O_2 is dimerization forming 5-5 diphenyl linkages and further polymerization of those dimers through formation of 4-O-5 linkages, mostly likely because of the generation of phenoxy radicals. Oxidative cleavage, however, is a minor pathway resulting in the formation of small quantities of aromatic aldehydes and alcohols (Figure 3).

Table 1. ^{1}H and ^{13}C NMR integration of the β-O-4 model substrate reaction products after treatment with Chelex.

^{1}H NMR	^{13}C NMR

Assignment	δ (ppm)	Integration	Assignment	δ (ppm)	Integration
OH$_{Ar}$	9.2 - 8.4	0.6	3',4',3,4	150.2 - 144.5	4.3
Aromatic	7.1 - 6.6	6.3	1	133.2	1.0
OH$_\beta$	5.5 - 5.2	0.9	5-5	128.2	0.4
α	4.9 - 4.7	1.0	1',6',6,5',5,2',2	122.8 - 109.0	7.4
OH$_\alpha$	4.7 - 4.5	0.8	β	84.9 - 81.7	1.0
β	4.5 - 4.3	1.0	α	73.6 - 69.8	1.0
OCH$_{3}$$_{+}$γ	3.9 - 3.5	7.5	OCH$_{3}$$_{+}$γ	63.3 - 52.1	3.2

Gel permeation chromatography analysis of Poplar organosolv lignin oxidation products.

Next, we evaluated the Mn-catalyzed oxidation of Poplar organosolv lignin by H_2O_2. To aid in product analysis, three samples were generated for comparison by GPC analysis: untreated organosolv lignin (i.e., untreated); organosolv lignin after treatment with Chelex (i.e, Chelex control); and the reaction products of Mn-catalyzed oxidation of organosolv lignin by H_2O_2 and subsequent treatment with Chelex (i.e., oxidized or treated). While, MALDI-TOF MS has been used to analyze the molecular weight distribution of lignin,[39, 40] the heterogeneous nature of lignin and its non-uniform repeat substructure makes the detailed oligomeric analysis conducted on the β-O-4 model substrate reaction products difficult, if not impossible. Thus, GPC analysis of acetylated lignin samples was used to determine the number-average molecular weight (M_n), weight-average molecular weight (M_w), and polydispersity index (PDI, indicates the width of the molecular weight distribution and is M_n/M_w).[41] The molecular weight distribution information resulting from GPC of lignin, though not absolute, can be used to compare changes in the lignin molecular weight distribution upon treatment with Chelex (to remove the Mn-catalyst) and/or oxidation by H_2O_2 activated by the Mn-catalyst.

GPC of the organosolv lignin and Chelex-treated organosolv lignin (Figure 5) show little change, although M_n does increase and the PDI decreases slightly for the control lignin sample upon Chelex treatment. This change in the M_n and PDI suggests that some of the low molecular

weight fraction of the untreated lignin molecular weight distribution is removed by Chelex. Although this small difference in molecular weight distribution may not be statistically significant and/or attributed to a normal variation in biological replicates, it would be consistent with the MALDI-TOF MS results that show some product removal after Chelex treatment (Figure S3). Upon oxidation by H_2O_2 activated by the Mn-catalyst, the treated lignin displays an approximate four-fold increase in M_n, a three-fold increase in M_w, and a two-fold increase in PDI, indicating that polymerization is occurring.
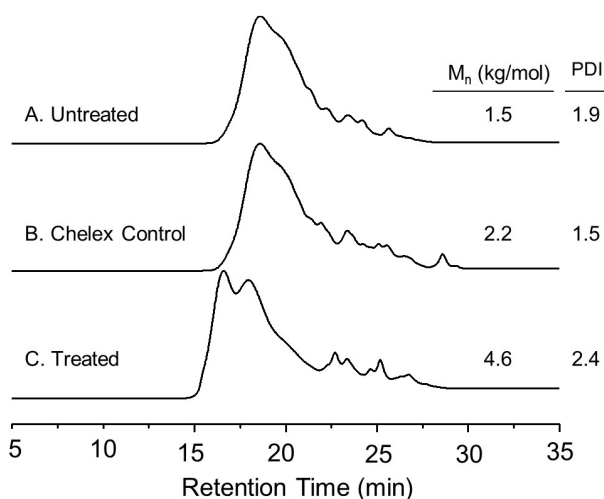

Figure 5. Gel permeation chromatograph of A. Poplar organosolv lignin, B. Chelex-treated control organosolv lignin, and C. reaction products of the Mn-catalyzed oxidation of organosolv lignin by H_2O_2 after Chelex treatment.

NMR analysis of Poplar organosolv lignin oxidation products.

^{1}H NMR can be employed to broadly profile and quantify the presence of lignin functional groups (e.g., carboxylic acids, formyl, aromatic, and methoxyl protons); however, hydroxyl groups cannot be readily measured. As a result, a method to quantitatively determine hydroxyl group distributions in lignin has been widely applied that relies on the *in situ* phosphitylation of lignin hydroxyl groups using 2–chloro–4,4,5,5–tetramethyl–1,3,2–dioxaphospholane (TMDP).[31]

The phosphorus atom that becomes adjacent and covalently linked to the oxygen atom of a lignin hydroxyl group and serves as a probe, generating resolvable ^{31}P NMR peaks that can be used to quantitatively profile aliphatic, syringyl (S), guaiacyl (G), *p*-hydroxyphenyl (H), and carboxylic hydroxyls. This type of ^{31}P NMR analysis does not give information on internal lignin monomer distribution, rather only the terminal lignin monomer distribution. However, it is particularly powerful in developing an understanding of lignin chain scission and condensation. Typically, hydrolysis of lignin inter-unit aryl ether linkages lead to a reduction in aliphatic hydroxyl content, along with an increase in phenolic content. ^{31}P NMR can also be used to detect C-C condensation at aromatic subunits that have terminal hydroxyls and C-O condensation at phenolic hydroxyls.

^{31}P NMR was used to analyze changes in organosolv lignin upon treatment with Chelex and/or oxidation by H_2O_2 activated by the Mn-catalyst (Figure 6). The mmol of lignin hydroxyl groups per g of lignin was quantified using the spectra shown in Figure 6 and the internal standard N-hydroxy-5-norbornene-2,3-dicarboximide (Table 2). There are some differences in the aromatic, carboxylic, and total hydroxyl group content upon treatment with Chelex when comparing the Chelex-treated and untreated lignin samples (both these samples are considered as controls because they were not exposed to H_2O_2 and Mn-catalyst).
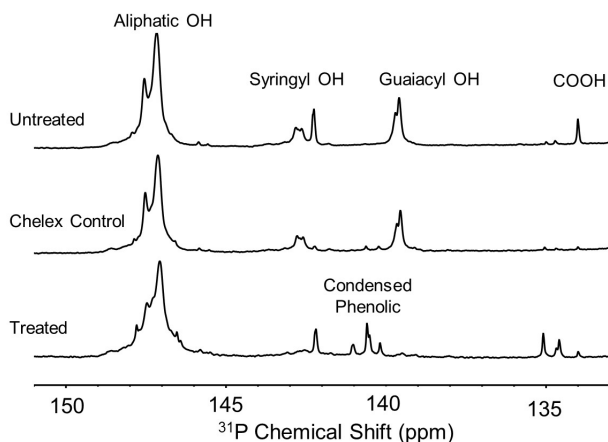

17

Figure 6: ^{31}P NMR of phosphorylated Poplar untreated organosolv lignin (top), control organosolv lignin after treatment with Chelex (middle), and reaction products of organosolv lignin oxidized by H_2O_2 activated by the Mn-catalyst followed by treatment with Chelex (bottom).

Though it is possible the Chelex resin chemically modified the untreated lignin, it is more likely that upon treatment with Chelex a chemically distinct fraction of lignin was removed. The GPC data of untreated and treated organosolv and MALDI-TOF MS data of β-O-4 model substrate reaction products supports this hypothesis. It could be that the low molecular weight lignin fraction removed by the Chelex arbitrarily contained lignin with a higher aromatic, carboxylic, and total hydroxyl content, or that Chelex selectively removes fractions with higher aromatic, carboxylic, and total hydroxyl contents, which in this case, just happened to also represent a low-molecular weight lignin fraction. Nevertheless, from this point on, the effect of oxidation by H_2O_2 activated by Mn-catalyst will be mainly elucidated by the comparison of control (i.e., Chelex treated) and oxidized lignin spectra.

Comparison of the ^{31}P NMR results from the control and oxidized lignin spectra show identical aromatic, aliphatic, and total hydroxyl contents, suggesting that neither chain scission at lignin inter-unit aryl ether linkages, nor chain condensation at aromatic hydroxyls is occurring. This is an important observation because of the significant amount of 4-O-5 condensation that occurs for the β-O-4 model substrate. The most important result of the ^{31}P NMR analysis is the complete shift of terminal guaiacyl hydroxyls that appear in the region from 140.0-138.0 ppm, to a series of peaks appearing at 141.5-140.0 ppm. The chemical shift region of 141.5-140.0 ppm has been

attributed to phosphorylated hydroxyl at 5-5 biphenyl groups,[31, 32] thus suggesting 5-5 biphenyl condensation is significant at terminal guaiacyl monomers.

Table 2. Hydroxyl concentrations of organosolv reaction products determined by ^{31}P NMR

Assignments	Chemical Shift Range (ppm)	Untreated (mmol OH/g lignin)	Chelex Control (mmol OH/g lignin)	Treated (mmol OH/g lignin)
Aliphatic OH	150.0-145.4	3.6	3.2	3.2
Aromatic OH	144.5-138.0	1.5	0.9	0.9
Carboxylic acid OH	135.5-132.5	0.1	0.0	0.2
Total OH		5.2	4.1	4.3
Syringyl OH	144.5-141.5	0.8	0.4	0.5
Condensed Phenol	141.5-140.0	0.0	0.0	0.4
Guaiacyl OH	140.0-138.0	0.7	0.5	0.0

Table 3. ^{13}C NMR integration of organosolv reaction products.

Assignment	δ (ppm)	Untreated /Aromatic Ring	Chelex Control /Aromatic Ring	Treated / Aromatic Ring
C_3/C_4 (G) & $C_3/C_4/C_5$ (S)	155-142	2.6	2.6	3.0
C_1 (G, S)	140-123	0.9	1.0	1.0
C_6 (G)	123-118	0.4	0.3	0.2
C_5 (G)	117-113	0.4	0.3	0.1
C_2 (G)	113-110	0.4	0.4	0.2
C_2/C_6 (S)	109-103	1.4	1.3	1.6

^{13}C NMR spectra of untreated, control, and treated samples are shown in Figure S8. Peak assignments and integration for the ^{13}C NMR spectrum of organosolv lignin reaction products are provided in Table 3 (peak assignments were made based on literature values[30]). The integration of specific functional groups was normalized by the aromatic carbon intensity in an effort to

account for variation in the lignin concentration within the NMR tube (which is difficult, if not impossible to control due to the highly variable solubility of lignin in DMSO). First, no peaks were observed above ~ 153 ppm, indicating that no oxidized carbon functional groups (i.e., aldehydes, esters, or carboxylic acids) were generated. On a qualitative level, 2D HSQC NMR suggests that oxidation has no effect on the lignin inter-unit linkages present (Figure S9). Second, the S/G ratio for the untreated and control lignin was ~ 1.8. In fact, the ^{13}C NMR results for the untreated and control lignin, unlike the ^{31}P NMR results, were remarkably similar. Next, there was no decrease in methoxy content detected for treated oxidized lignin when compared to untreated and control lignin, further suggesting that 4-O-5 formation does not occur in the organosolv lignin. Lastly, the ^{13}C NMR spectral intensity typically associated with G subunits shifts to chemical shift regions associated with S subunits. It is unlikely S subunits are being generated; what is more likely is that as condensation at 5-postions on the G subunits occur so that its aromatic carbon chemical shift more resembles that of the aromatic carbon chemical shift of S subunits (which have both 3- and 5-postion occupied by electron withdrawing methoxy groups).

Conclusions

In contrast to fungal manganese peroxidases that degrade lignin, our study shows the Mn catalyst's peroxidative oxidation of the β-O-4 lignin model substrate and organosolv lignin resulted primarily in polymerization with small amounts of substrate cleavage. The polymerization reaction took place faster than the subsequent oxidations that would have promoted lignin cleavage at β-O-4 linkages thus, highlighting the complexity of oxidative strategies to generate small aromatic compounds via lignin oxidative enzymatic degradation. However as evinced by NMR, the syringyl subunits of the organosolv lignin did not condense,

suggesting interesting possibilities in lignin bio-depolymerization strategies. In our opinion, possibilities could include expanding current genetic engineering of biomass sources to included producing lignin that consists primarily of syringyl subunits. Without the 5-postion on the aromatic ring of the lignin monomer available for polymerization, the predominate pathway could shift to lignin degradation. Alternatively, enzymatic-catalyzed depolymerization of lignin in continuous-flow reactors with oxidative enzymes could facilitate higher yields of small aromatic compounds due to the reduced residence time of fragmented moieties in the reactor or that are in the vicinity of the macromolecular lignin. Lignin remains an important source of aromatic carbon that is currently under-utilized due to the difficulty in breaking it down in a way that gives clean reaction products that can be easily refined. However, the effort expended on the difficult problem of lignin de-polymerization could result in a renewable non-petroleum based source for fuels and fine chemicals.

Associated content

Two methods, one scheme, one table and 9 figures. This material is available free of charge via the internet at http://pubs.acs.org.

Author information

*Corresponding Authors

butler@chem.ucsb.edu

mfoston@wustl.edu

Notes

References

1.   Tilman, D.; Socolow, R.; Foley, J. A.; Hill, J.; Larson, E.; Lynd, L.; Pacala, S.; Reilly, J.; Searchinger, T.; Somerville, C.; Williams, R., Beneficial biofuels-the food, energy, and environment trilemma. *Science (Washington, DC, U. S.)* **2009,** *325*, (5938), 270-271.

2.   Azadi, P.; Inderwildi, O. R.; Farnood, R.; King, D. A., Liquid fuels, hydrogen and chemicals from lignin: A critical review. *Renewable Sustainable Energy Rev.* **2013,** *21*, 506-523.

3.   Lange, H.; Decina, S.; Crestini, C., Oxidative upgrade of lignin - Recent routes reviewed. *Eur. Polym. J.* **2013,** *49*, (6), 1151-1173.

4.   Liu, W.-J.; Jiang, H.; Yu, H.-Q., Thermochemical conversion of lignin to functional materials: a review and future directions. *Green Chemistry* **2015,** *17*, (11), 4888-4907.

5.   Simmons, B. A.; Loque, D.; Ralph, J., Advances in modifying lignin for enhanced biofuel production. *Curr. Opin. Plant Biol.* **2010,** *13*, (3), 313-320.

6.   De Wild, P. J.; Huijgen, W. J. J.; Gosselink, R. J. A., Lignin pyrolysis for profitable lignocellulosic biorefineries. *Biofuels, Bioprod. Biorefin.* **2014,** *8*, (5), 645-657.

7.   Ma, Z.; Custodis, V.; van Bokhoven, J. A., Selective deoxygenation of lignin during catalytic fast pyrolysis. *Catal. Sci. Technol.* **2014,** *4*, (3), 766-772.

8.   Ragauskas, A. J.; Beckham, G. T.; Biddy, M. J.; Chandra, R.; Chen, F.; Davis, M. F.; Davison, B. H.; Dixon, R. A.; Gilna, P.; Keller, M.; Langan, P.; Naskar, A. K.; Saddler, J. N.; Tschaplinski, T. J.; Tuskan, G. A.; Wyman, C. E., Lignin Valorization: Improving Lignin Processing in the Biorefinery. *Science (Washington, DC, U. S.)* **2014,** *344*, (6185), 709.

9.   Himmel, M. E.; Ding, S.-Y.; Johnson, D. K.; Adney, W. S.; Nimlos, M. R.; Brady, J. W.; Foust, T. D., Biomass Recalcitrance: Engineering Plants and Enzymes for Biofuels Production. *Science (Washington, DC, U. S.)* **2007,** *315*, (5813), 804-807.

10.   Nguyen, B. H.; Perkins, R. J.; Smith, J. A.; Moeller, K. D., Solvolysis, Electrochemistry, and Development of Synthetic Building Blocks from Sawdust. *J. Org. Chem.* **2015,** *80*, (24), 11953-11962.

11.   Vanholme, R.; Demedts, B.; Morreel, K.; Ralph, J.; Boerjan, W., Lignin biosynthesis and structure. *Plant Physiol.* **2010,** *153*, (3), 895-905.

12.   Ding, S.-Y.; Liu, Y.-S.; Zeng, Y.; Himmel, M. E.; Baker, J. O.; Bayer, E. A., How Does Plant Cell Wall Nanoscale Architecture Correlate with Enzymatic Digestibility? *Science (Washington, DC, U. S.)* **2012,** *338*, (6110), 1055-1060.

13.   Hofrichter, M.; Ullrich, R.; Pecyna, M. J.; Liers, C.; Lundell, T., New and classic families of secreted fungal heme peroxidases. *Appl. Microbiol. Biotechnol.* **2010,** *87*, (3), 871-897.

14.   Pollegioni, L.; Tonin, F.; Rosini, E., Lignin-degrading enzymes. *FEBS J.* **2015,** *282*, (7), 1190-1213.

15.   Vares, T.; Hatakka, A., Lignin-degrading activity and ligninolytic enzymes of different white-rot fungi: effects of manganese and malonate. *Canadian Journal of Botany* **1997,** *75*, (1), 61-71.

16.   Wariishi, H.; Dunford, H. B.; MacDonald, I. D.; Gold, M. H., Manganese peroxidase from the lignin-degrading basidiomycete Phanerochaete chrysosporium. Transient state kinetics and reaction mechanism. *J. Biol. Chem.* **1989,** *264*, (6), 3335-40.

17.   Kirk, T. K.; Connors, W. J.; Bleam, R. D.; Hackett, W. F.; Zeikus, J. G., Preparation and microbial decomposition of synthetic [14C]ligins. *Proceedings of the National Academy of Sciences* **1975,** *72*, (7), 2515-2519.

18.   Kirk, T. K.; Connors, W. J.; Zeikus, J. G., Requirement for a Growth Substrate During Lignin Decomposition by Two Wood-Rotting Fungi. *Applied and Environmental Microbiology* **1976,** *32*, (1), 192-194.

19.   Liers, C.; Arnstadt, T.; Ullrich, R.; Hofrichter, M., Patterns of lignin degradation and oxidative enzyme secretion by different wood- and litter-colonizing basidiomycetes and ascomycetes grown on beech-wood. *FEMS Microbiol. Ecol.* **2011,** *78*, (1), 91-102.

20.   Tuor, U.; Wariishi, H.; Schoemaker, H. E.; Gold, M. H., Oxidation of phenolic arylglycerol β-aryl ether lignin model compounds by manganese peroxidase from Phanerochaete chrysosporium: oxidative cleavage of an α-carbonyl model compound. *Biochemistry* **1992,** *31*, (21), 4986-95.

21.   Crestini, C.; Pastorini, A.; Tagliatesta, P., Metalloporphyrins immobilized on montmorillonite as biomimetic catalysts in the oxidation of lignin model compounds. *J. Mol. Catal. A: Chem.* **2004,** *208*, (1-2), 195-202.

22.   Crestini, C.; Pastorini, A.; Tagliatesta, P., The immobilized porphyrin-mediator system Mn(TMePyP)/clay/HBT (clay-PMS): A lignin peroxidase biomimetic catalyst in the oxidation of lignin and lignin model compounds. *Eur. J. Inorg. Chem.* **2004**, (22), 4477-4483.

23.   Biannic, B.; Bozell, J. J., Efficient Cobalt-Catalyzed Oxidative Conversion of Lignin Models to Benzoquinones. *Org. Lett.* **2013,** *15*, (11), 2730-2733.

24.   Cedeno, D.; Bozell, J. J., Catalytic oxidation of para-substituted phenols with cobalt–Schiff base complexes/O2—selective conversion of syringyl and guaiacyl lignin models to benzoquinones. *Tetrahedron Letters* **2012,** *53*, (19), 2380-2383.

25.   Salanti, A.; Orlandi, M.; Tolppa, E.-L.; Zoia, L., Oxidation of isoeugenol by salen complexes with bulky substituents. *Int. J. Mol. Sci.* **2010,** *11*, 912-926.

26.   Chang, S.; Galvin, J. M.; Jacobsen, E. N., Effect of Chiral Quaternary Ammonium Salts on (salen)Mn-Catalyzed Epoxidation of cis-Olefins. A Highly Enantioselective, Catalytic Route to Trans-Epoxides. *Journal of the American Chemical Society* **1994,** *116*, (15), 6937-6938.

27.   Björkstén, F., A Kinetic Study of the Horse-Radish Peroxidase-Catalyzed Oxidation of Iodide. *European Journal of Biochemistry* **1968,** *5*, (1), 133-142.

28.   Samuel, R.; Pu, Y.; Raman, B.; Ragauskas, A. J., Structural characterization and comparison of switchgrass ball-milled lignin before and after dilute acid pretreatment. *Appl. Biochem. Biotechnol.* **2010,** *162*, (1), 62-74.

29.   Kim, H.; Ralph, J., Solution-state 2D NMR of ball-milled plant cell wall gels in DMSO-d6/pyridine-d5. *Org. Biomol. Chem.* **2010,** *8*, (3), 576-591.

30.   Capanema, E. A.; Balakshin, M. Y.; Kadla, J. F., Quantitative Characterization of a Hardwood Milled Wood Lignin by Nuclear Magnetic Resonance Spectroscopy. *J. Agric. Food Chem.* **2005,** *53*, (25), 9639-9649.

31.   Pu, Y.; Cao, S.; Ragauskas, A. J., Application of quantitative 31P NMR in biomass lignin and biofuel precursors characterization. *Energy Environ. Sci.* **2011,** *4*, (9), 3154-3166.

32.   Crestini, C.; Sermanni, G. G.; Argyropoulos, D. S., Structural modifications induced during biodegradation of wheat lignin by Lentinula edodes. *Bioorg. Med. Chem.* **1998,** *6*, (7), 967-973.

33.   Boyle, C. D.; Kropp, B. R.; Reid, I. D., Solubilization and mineralization of lignin by white rot fungi. *Appl. Environ. Microbiol.* **1992,** *58*, (10), 3217-24.

34.   Kerem, Z.; Hadar, Y., Effect of manganese on preferential degradation of lignin by Pleurotus ostreatus during solid-state fermentation. *Appl. Environ. Microbiol.* **1995,** *61*, (8), 3057-62.

35.   Gierer, J., Formation and involvement of superoxide (O2·-/HO2.) and hydroxyl (OH·) radicals in TCF bleaching processes. A review. *Holzforschung* **1997,** *51*, (1), 34-46.

36.   Haikarainen, A.; Sipila, J.; Pietikainen, P.; Pajunen, A.; Mutikainen, I., Salen complexes with bulky substituents as useful tools for biomimetic phenol oxidation research. *Bioorg. Med. Chem.* **2001,** *9*, (6), 1633-1638.

37.   Areskogh, D.; Li, J.; Nousiainen, P.; Gellerstedt, G.; Sipilae, J.; Henriksson, G., Oxidative polymerization of models for phenolic lignin end-groups by laccase. *Holzforschung* **2010,** *64*, (1), 21-34.

38.   Ralph, S. A., Landucci, L. L., Ralph, J., NMR Database of Lignin and Cell Wall Model Compounds; available over the internet at http://ars.usda.gov/Services/docs.htm?docid)10429. In 2004.

39.   Metzger, J. O.; Bicke, C.; Faix, O.; Tuszynski, W.; Angermann, R.; Karas, M.; Strupat, K., Matrix-Assisted Laser Desorption Mass Spectrometry of Lignins**. *Angewandte Chemie International Edition in English* **1992,** *31*, (6), 762-764.

40.   Banoub, J. H.; Delmas, M., Structural elucidation of the wheat straw lignin polymer by atmospheric pressure chemical ionization tandem mass spectrometry and matrix-assisted laser desorption/ionization time-of-flight mass spectrometry. *Journal of Mass Spectrometry* **2003,** *38*, (8), 900-903.

41.   Tolbert, A.; Akinosho, H.; Khunsupat, R.; Naskar, A. K.; Ragauskas, A. J., Characterization and analysis of the molecular weight of lignin for biorefining studies. *Biofuels, Bioprod. Biorefin.* **2014,** *8*, (6), 836-856.

TOC Figure and Synopsis

Peroxidative Oxidation of Lignin and a Lignin Model Compound by a Manganese SALEN Derivative

Stephen D. Springer, Jian He, Megan Chui, R. Daniel Little, Marcus Foston, and Alison Butler
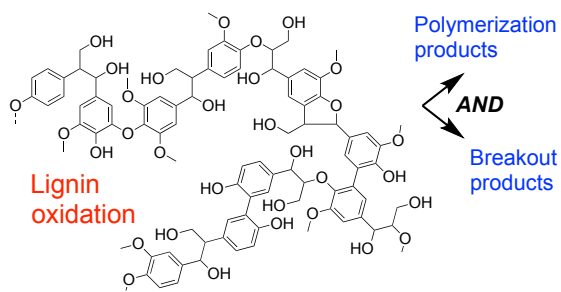
Synopsis

A MnSALEN derivative catalyzes oxidation of organosolv lignin and a model substrate by H_2O_2 producing breakout products as well as further polymerization.